Vol. 47, No. 2 (2025) 228-249, DOI: 10.24874/ti.1842.12.24.03

Tribology in Industry

www.tribology.rs

RESEARCH

# Multi-Objective Optimization in Hard Turning of AISI 4140 Steel Using Taguchi-Based GRA and DEAR with Ceramic Tool

Mohand Ouidir Sahbi[a,*], Sadeddine Abdelhamid[a], Mohamed Athmane Yallese[b], Salim Belhadi[b], Abdelatif Belamri[a]

[a]*Université de Bejaia, Faculté de Technologie, Laboratoire de Mécanique, Matériaux et Énergétique (L2ME), 06000 Bejaia, Algeria,*
[b]*Laboratory of Mechanics and Structure (LMS), Department of Mechanical Engineering, University 8 May 1945, P.O. Box 401, 24000 Guelma, Algeria.*

Keywords:

*Hard machining*
*AISI 4140*
*Ceramics*
*Tool-wear*
*Surface roughness*
*MCDM Optimization*

* Corresponding author:

*Mohand Ouidir Sahbi*
*E-mail:*
*mohandouidir.sahbi@univ-bejaia.dz*

*Received: 26 December 2024*
*Revised: 3 February 2025*
*Accepted: 24 March 2025*

A B S T R A C T

*In machining, achieving a low surface roughness (Ra), minimal tool wear (VB), and a high material removal rate (MRR) is essential for successful hard turning. This study investigates the optimal cutting conditions for hard turning of AISI 4140 steel using a Taguchi $L_9$ experimental design. Four factors were varied: cutting speed (Vc), feed rate (f), depth of cut (Doc), and cutting tool material (mixed ceramic CC650, TiN-coated mixed ceramic CC6050, and composite ceramic CC670). The experimental results were carefully measured after each test, and ANOVA was performed to analyze the influence of input parameters on the output variables. A multi-objective optimization was applied using Grey Relational Analysis (GRA) and Data Envelopment Analysis Ranking (DEAR) based on Taguchi analysis to simultaneously minimize Ra and VB while maximizing MRR. The results revealed that the optimal regimes produce Ra and VB values below their minimum levels. The DEAR method achieves a higher MRR compared to GRA. The CC6050 insert demonstrated superior performance in terms of Ra and VB. The optimal conditions identified by GRA and DEAR maintained f = 0.08 mm/rev, Doc = 0.3 mm, and the CC6050 insert, with a variation in cutting speed (Vc). ANOVA results for surface roughness (Ra) revealed that the feed rate (f) had the most significant influence, contributing 82.35% to Ra. Vc had the most significant influence on VB, contributing 37.03%. Among the tested inserts, CC6050 exhibited the lowest wear (VB = 0.09 mm), followed by CC670 (VB = 0.18 mm).*



## 1. INTRODUCTION

Recently, hard turning has progressed with advances in cutting tool technology, machine tool capabilities, and the optimization of machining processes, leading to the introduction of new high-performance materials offering better wear resistance and greater

thermal stability [1,2]. The most frequent problem in this type of machining lies in the choice of cutting tools that overcome wear issues and ensure better productivity and quality of machined surfaces [3]. Ceramic tools, characterized by their strength and hardness, are among the cutting materials most commonly used to meet the desired objectives and have been the subject of much research [4,5]. This study aims to identify the optimum combination that maximizes machining efficiency, improves tool life, and ensures increased productivity.

Due to these characteristics, ceramic tools are suitable for hard machining material such as AISI 4140 steel, which is widely used in many industrial applications, including shafts, driving pins, and gears [6]. A lot of work has been published on the machining of this material. Saikaew et al. [7] evaluated the machining performance of coated WC inserts and ceramic inserts for turning AISI 4140 steel. Their results show a significant influence of cutting speed and insert type on surface roughness and tool wear. A cutting speed of 220 m/min is optimal, and wear is more pronounced for coated WC inserts than for ceramic ones.

Kim et al. [8] examined the effect of machinability on surface quality and vibration during hard turning of heat-treated AISI 4140 steels, using ceramic cutting tools in a dry environment. The results show that surface quality and vibration are influenced by the feed rate, which is the most critical parameter. Ahmed et al. [9] studied and optimized the machining of AISI 4140 steel using a self-propelled rotary tool. The input parameters included cutting speed, feed rate, and rake angle, whereas the output parameters were surface roughness, tool wear, and material removal rate. Padhan et al. [10] studied the machining of hardened AISI 4140 steels with a coated carbide tool under nanofluid-MQL and showed that the feed had the most significant impact (58.18%) on surface roughness, followed by the nose radius (12.32%) and the speed (0.85%). Asilturk et al. [11] used fuzzy machine learning to analyze the effect of cutting parameters on vibrations, surface roughness, and acoustic emissions during the dry turning of AISI 4140 steel. The results contribute to a deeper understanding of the impact of machining conditions on this material. Awadh et al. [12] conducted a comparison of the machinability of three types of coated carbide inserts for hard turning of AISI 4340 steel, evaluating factors such as roughness, noise, energy consumption, and cutting forces. They used grey relational analysis optimization coupled with the Crow search algorithm to determine the best cutting parameters. Sudhansu et al. [13] studied the dry machining of AISI 4140 steel using TiN-coated ceramic inserts. The results indicate that feed rate is the main parameter influencing surface roughness, followed by cutting speed. Flank wear, on the other hand, is mainly affected by cutting speed and the interaction between feed rate and depth of cut.

Among the many input parameters used to evaluate these processes, some have divergent objectives. Consequently, several multi-criteria optimization methods, namely GRA, MOORA, DEAR, etc., are effective in determining optimal machining regimes and have several practical applications [14].

Over the last few years, a number of studies have made effective use of these methods for machining various materials. Table 1 summarizes some of the work carried out in relation to these optimization methods.

The combined Taguchi-GRA and DEAR approach is expected to enhance the efficiency of machining process optimization. A thorough review of the literature shows that several investigations have been carried out into the optimization of machining processes using Taguchi-GRA and DEAR methods. However, there are very few studies that look at using MCDM tools to optimize different technological parameters in the machining of AISI 4140 while considering various input factors in hard turning. In addition, existing approaches do not always take into account the cutting tool material as an input parameter.

To overcome these shortcomings, this study optimizes the machining of AISI 4140 steel using a combination of DEAR and GRA methods with Taguchi (S/N) analysis. The study simultaneously evaluates the influence of four input parameters on three output parameters to improve process efficiency while comparing the performance of three high-performance ceramic tools.

**Table 1.** Recent optimizations studies.

| Authors | Optimization methods | Optimization objectives | Machining process | Workpiece material |
|---|---|---|---|---|
| Chate et al. [15] | Taguchi, MOORA and DEAR | Material removal rate MRR, surface roughness SR and circularity error CE | Turning | Mild steel |
| Ponugoti et al. [16] | GRA and PCA | Machining force, SR and surface temperature | Turning | AISI 52100 |
| Safi et al. [17] | GRA, DEAR, MOORA and WASPAS | Cutting force Fz, SR, cutting power Pc and MRR | Turning | X210Cr12 |
| Hadjela et al. [18] | Taguchi, GRA, TOPSIS and MOORA | Tool wear, SR and MRR | Turning | AISI 4140 |
| Umamaheswarrao et al. [19] | Hybrid GRA-PCA | Surface quality, Machining force and workpiece temperature | Turning | AISI 52100 |
| Khelfaoui et al. [20] | Taguchi- GRA | Tool wear, SR and cutting temperature | Turning | AISI D3 |
| Meral et al. [21] | Taguchi-GRA | Thrust force Fz, SR and drilling torque | Drilling | AISI 4140 |
| Patole et al. [22] | GRA | Cutting force and SR | Turning | AISI 4340 |
| Nagwa et al. [23] | GRA | Tool life, SR and MRR | Turning | AISI 420 |
| Rao et al. [24] | Taguchi, GRA and TOPSIS | Tool wear, SR and MRR | Turning | Inconel 718 |
| Sultana et al. [25] | Hybrid GRA-PCA | Chip tool interface temperature, arithmetic surface roughness Ra and specific cutting energy Esp | Turning | AISI 1040 |
| Kumar et al. [26] | GRA | Tool wear, SR and cutting temperature | Turning | AISI D3 |
| Upadhyay et al. [27] | GRA | Cutting force, SR and MRR | Turning | AISI 4140 |
| Yaqoob et al. [28] | Taguchi-GRA | Tool life and SR | Turning | AISI 4340 |
| Rameswara et al. [29] | Taguchi-GRA | SR and MRR | Turning | AISI 1045 |
| Hong et al. [30] | DEAR | Cutting forces and MRR | Turning | AISI 1055 |
| Pathapalli et al. [31] | Taguchi-GRA and DERA | SR and MRR | Abrasive water-jet machining (AWJM) | Ti6Al4V |
| Imran et al. [32] | GRA, DEAR and MOORA | SR and MRR | Turning | Mild steel |

To achieve these objectives, this article is structured in five main parts: After an introduction and a literature review covering the research work on machining of AISI 4140 steel and optimization methods, the second section describes the materials, methods used, and the experimental design applied. The third section presents the various results obtained, accompanied by a discussion analyzing these findings. The fourth section discusses the optimization methods adopted, both single-objective and multi-objective (GRA and DEAR). Finally, the article concludes with the main results and perspectives for future research.

## 2. EXPERIMENTAL PROCEDURE

A hard machining process is adapted in this study on AISI 4140 steel. A chromium-molybdenum steel, mainly used in mechanical manufacturing, particularly for the production of large cross-section parts, crankshafts, gears, etc. [6,9]. Table 2 details the chemical and mechanical properties of this steel. The part has a diameter of 60 mm, a length of 185 mm, and a machining length of 150 mm. A mixed fixture clamped the part on a conventional lathe with a power of 6.6 kW. Machining operations were carried out using three types of SANDVIK ceramic cutting inserts: uncoated mixed ceramic (T1/CC650), TiN-coated

mixed ceramic (T2/CC6050), and composite ceramic (T3/CC670). The choice of these ceramic inserts is based on their high machining performance, characterized by their high hardness, excellent wear resistance, and thermal stability, which makes it a favorable choice for hard machining [33]. They are held in place by specific toolholders; the PSBNR 2525M12 dedicated to the T1 and T2 inserts, while the CSBNR 2525M12 toolholder is used for the T3 insert. These inserts share a common tool geometry, defined by the following angles: $\chi r$=+75°, $\alpha$=+6°, $\gamma$=-6°, $\lambda$=-6°. Table 3 shows the characteristics of these inserts.

**Table 2.** Chemical composition and mechanical properties of AISI 4140.

| **Chemical composition [%]** | | | | | | | | | |
|---|---|---|---|---|---|---|---|---|---|
| C | Si | Mn | P | S | Cr | Ni | Mo | Al | Cu |
| 0.421 | 0.227 | 0.756 | 0.011 | 0.023 | 1.05 | 0.154 | 0.16 | 0.02 | 0.175 |
| **Mechanical properties** | | | | | | | | | |
| Young's modulus E (Mpa) | | | | | 210*10³ | | | | |
| Yield strength Re (Mpa) | | | | | 755 | | | | |
| Tensile strength Rm (Mpa) | | | | | 886 | | | | |
| Hardness (HRC) | | | | | 52 | | | | |

**Table 3.** Characteristics of cutting insert used.

| | **Uncoated mixed ceramic CC650** | **Coated mixed ceramic CC6050** | **Composite ceramic CC670** | **Insert design** |
|---|---|---|---|---|
| **Designation** | SNGA 12-04-08 T01020 | SNGA 12-04-08 S01525 | SNGN 12-04-08 T01020 | |
| **Cutting insert** |   |   |   | 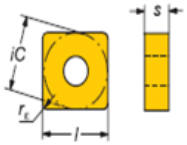  |
| **Compositions** | 70% Al2O2+30% TiC | 70% Al2O2+30% Tic coated with TiN | 75% Al2O3+25% Sic | |
| **Tool holder** | PSBNR 2525M 12 | | CSBNR 25250M 12 | |

Surface roughness (Ra) was measured using a roughness tester (Surftest 210 Mitutoyo) placed directly on the lathe, without dismantling the part along the line corresponding to the radius of the part, while keeping it parallel to the axis of rotation and aligned with the surface being measured to ensure a representative and reliable measurement. The device has a measuring range of 17.5 mm and exerts a displacement force of 4 mN. It is fitted with a diamond probe with a 5 µm tip radius, which moves linearly over the measured surface a resolution and a resolution f 0.1 µm with Gaussian filter. The probe length is 4 mm, with a base length of 0.8 mm (0.8 × 5). The measurement range for roughness criteria is between 0.05 and 40 µm [34]. Each measurement is the average of three tests done on the machined part, spaced 120° to ensure a representative assessment of the surface condition.

The wear (VB) of the cutting inserts was meticulously assessed using a Visual Gage 250 microscope, specially designed for metrology and surface analysis. The microscope is equipped with a high-resolution camera for precise image capture of the wear surface, as well as an optical magnification system connected to a computer and controlled by Visual Gage 2.2.0 software.

Figure 1 shows the experimental set-up used in our study, starting with the machining process, followed by the measurement of the various output parameters to carry out the ANOVA and finally the optimization.

The material removal rate (MRR) is the amount of material taken away per unit of time ($mm^3$/min) for each cycle of the experiment. It is found using equation (1) [35].

$$MRR = Vc[m/min] \times f[mm/rev] \times Doc[mm] \times 1000 \quad (1)$$

Experiments were carried out using the Taguchi $L_9$ experimental design (3^4), also known as the orthogonal array that can significantly reduce the number of tests by minimizing the effects of uncontrollable variables. This method involves four cutting variables at three levels, leading to a total of nine trials. The selected cutting parameters were influenced by earlier research on hard machining of AISI 4140 steel [4] and were within the ranges recommended by the Sandvik cutting insert manufacturer [36]. Most studies suggested depths of cut of 0.1 to 1 mm, feeds of 0.05 to 0.25 mm/rev, and cutting speeds exceeding 75 m/min. Three levels are defined for each cutting variable. Table 4 displays the factors studied and their corresponding level designations.

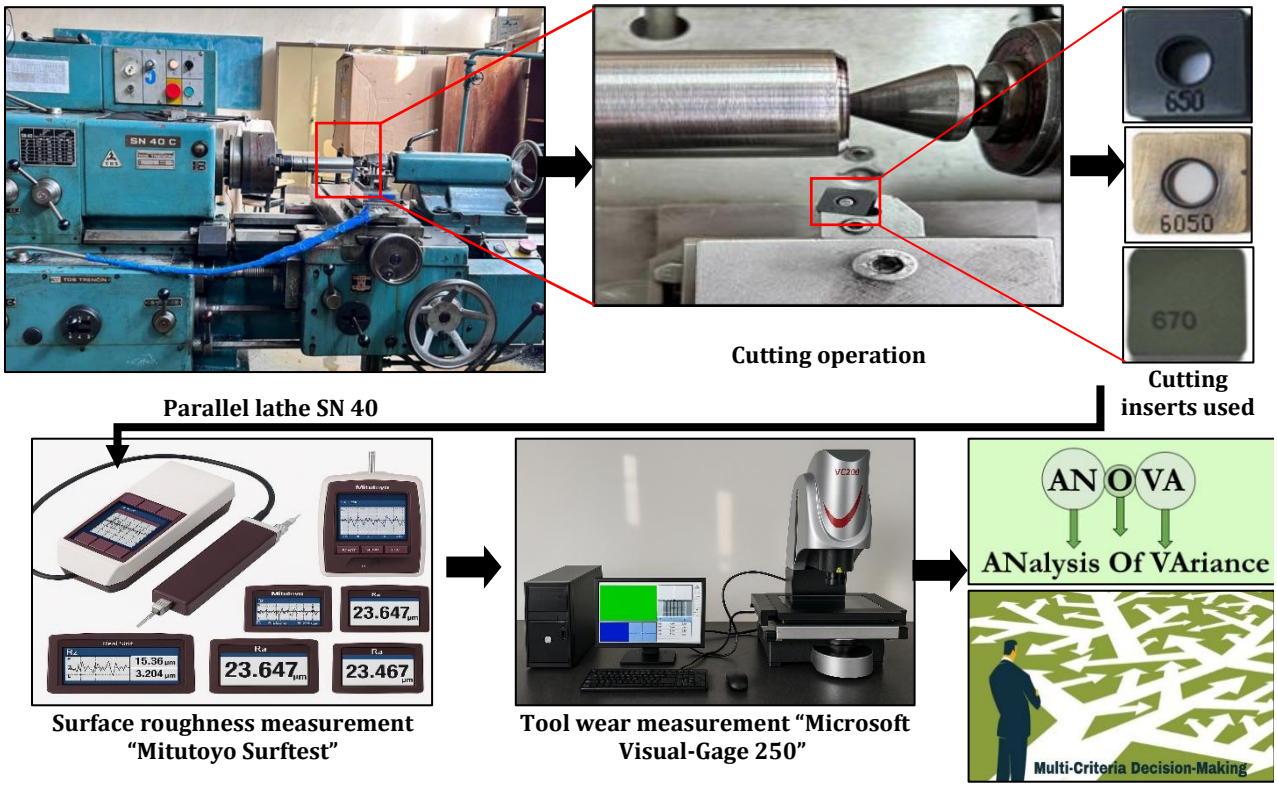


**Fig. 1.** Graphical illustration of the experimental study.

**Table 4.** Taguchi $L_9$ experimental design (3^4).

| N° Test | Material | Vc | f | Doc |
|---|---|---|---|---|
| **1** | 1 | 1 | 1 | 1 |
| **2** | 1 | 2 | 2 | 2 |
| **3** | 1 | 3 | 3 | 3 |
| **4** | 2 | 1 | 2 | 3 |
| **5** | 2 | 2 | 3 | 1 |
| **6** | 2 | 3 | 1 | 2 |
| **7** | 3 | 1 | 3 | 2 |
| **8** | 3 | 2 | 1 | 3 |
| **9** | 3 | 3 | 2 | 1 |

## 3. RESULTS AND DISCUSSIONS

For each of the nine tests carried out, the response data, including Ra, VB and MRR, were precisely measured, calculated and recorded in Table 5. The variation in the four input factors Vc (m/min), f (mm/rev), Doc (mm) and the tool material (Ti) are also given. The values of the different measured outputs (Ra, VB) and the calculated parameters (MRR) vary successively within the ranges of (0.492 to 1.203 µm), (0.09 to 0.43 mm) and (800 to 12480 $mm^3$/min) respectively.

**Table 5.** Taguchi $L_9$ experimental tests results.

| N° Test | Material | Vc (m/min) | f [mm/tr] | Doc [mm] | Ra [µm] | VB [mm] | MRR [mm³/min] |
|---|---|---|---|---|---|---|---|
| **1** | T1 | 100 | 0.08 | 0.1 | 0.592 | 0.1 | 800 |
| **2** | T1 | 180 | 0.12 | 0.2 | 0.783 | 0.21 | 4320 |
| **3** | T1 | 260 | 0.18 | 0.3 | 1.203 | 0.43 | 12480 |
| **4** | T2 | 100 | 0.12 | 0.2 | 0.62 | 0.09 | 3660 |
| **5** | T2 | 180 | 0.16 | 0.3 | 1.11 | 0.11 | 2880 |
| **6** | T3 | 260 | 0.08 | 0.1 | 0.589 | 0.14 | 4160 |
| **7** | | 100 | 0.16 | 0.3 | 1.016 | 0.11 | 3200 |
| **8** | T3 | 180 | 0.08 | 0.1 | 0.492 | 0.12 | 4320 |
| **9** | T3 | 260 | 0.12 | 0.2 | 0.998 | 0.18 | 3120 |

### 3.1 Analyze of variance ANOVA

The experimental results for roughness Ra and wear VB were subjected to ANOVA to observe the effect of machining parameters on the experimental results and to directly quantify the influence of each factor on the variations of the given response. The results of the ANOVA performed at the 5 % significance level are presented in Tables 6 and 7 for VB and Ra and no ANOVA analysis is performed for the MRR, as it is calculated according to Equation 1. For each combination, the effects of the three parameters Vc (m/min), f (mm/rev) and Doc (mm) as well as the tool material were examined. The last column of each table represents the percentage contribution of each input parameter, providing an overview of the degree of impact of the input factors on output parameters.

**Table 6.** ANOVA for VB.

| Source | SS | DF | MS | F-value | p-value | Contribution [%] |
|---|---|---|---|---|---|---|
| **Model** | 0.0886 | 5 | 0.0177 | 22 | 0.0143 | 97.36 |
| **Material** | 0.0304 | 2 | 0.0152 | 18.88 | 0.02 | 33.41 |
| **Vc [m/min]** | 0.0337 | 1 | 0.0337 | 41.9 | 0.0075 | 37.03 |
| **f [mm/rev]** | 0.014 | 1 | 0.014 | 17.4 | 0.0251 | 15.38 |
| **Doc [mm]** | 0.0104 | 1 | 0.0104 | 12.93 | 0.0369 | 11.43 |
| **Residual** | 0.0024 | 3 | 0.0008 | | | |
| **Cor Total** | 0.091 | 8 | | | | |

**Table 7.** ANOVA for Ra.

| Source | SS | DF | MS | F-value | p-value | Contribution [%] |
|---|---|---|---|---|---|---|
| **Model** | 0.5463 | 5 | 0.1093 | 37.2 | 0.0067 | 98.41 |
| **Material** | 0.0119 | 2 | 0.006 | 2.03 | 0.2772 | 2.14 |
| **Vc [m/min]** | 0.0526 | 1 | 0.0526 | 17.92 | 0.0241 | 9.48 |
| **f [mm/rev]** | 0.4571 | 1 | 0.12 | 155.59 | 0.0011 | 82.35 |
| **Doc [mm]** | 0.0247 | 1 | 0.0247 | 8.41 | 0.0011 | 82.35 |
| **Residual** | 0.0088 | 3 | 0.0029 | | | |
| **Cor Total** | 0.55513 | 8 | | | | |

**Table 8.** ANOVA for Ra after pooling out the Ti.

| Source | SS | DF | MS | F-value | p-value | Contribution [%] |
|---|---|---|---|---|---|---|
| **Model** | 0.5344 | 3 | 0.178134 | 42.97 | 0.001 | 96.26 |
| **Vc [m/min]** | 0.05264 | 1 | 0.052641 | 12.70 | 0.016 | 9.48 |
| **f [mm/rev]** | 0.45706 | 1 | 0.457056 | 110.25 | 0.000 | 82.38 |
| **Doc [mm]** | 0.02470 | 1 | 0.024704 | 5.96 | 0.059 | 4.45 |
| **Residual** | 0.02073 | 5 | 0.004145 | | | |
| **Cor Total** | 0.55513 | 8 | | | | |

**Table 9.** ANOVA for Ra after pooling out the Doc.

| Source | SS | DF | MS | F-value | p-value | Contribution [%] |
|---|---|---|---|---|---|---|
| **Model** | 0.50970 | 2 | 0.254848 | 33.66 | 0.001 | 91.82 |
| **Vc [m/min]** | 0.05264 | 1 | 0.052641 | 6.95 | 0.039 | 9.48 |
| **f [mm/rev]** | 0.45706 | 1 | 0.457056 | 60.36 | 0.000 | 82.38 |
| **Residual** | 0.04543 | 6 | 0.007572 | | | |
| **Cor Total** | 0.55513 | 8 | | | | |

Table 6 shows the ANOVA for wear (VB). All the input parameters significantly influence the change in VB. The factor Vc (m/min) has the most impact on this response, accounting for 37.03 % of the change. It is followed by the cutting tool material factor, which accounts for 33.41 % of the change. This finding confirms how the wear's progression is significantly influenced by the physical and mechanical properties of the tool material; the same results are presented in the work of Selvaraj et al. [37]. Finally, the feed rate f (mm/rev) and Doc (mm) each account for 15.38% and 11.43 %, respectively. The ANOVA results in the following modelling Equations 2, 3 and 4 for the three cutting tools T1, T2 and T3, respectively:

$$VB_{(T1)} = -0.15 + 0.0009 \times Vc + 1.2 \times f + 0.42 \times Doc \quad (2)$$

$$VB_{(T2)} = -0.28 + 0.0009 \times Vc + 1.2 \times f + 0.42 \times Doc \quad (3)$$

$$VB_{(T2)} = -0.26 + 0.0009 \times Vc + 1.2 \times f + 0.42 \times Doc \quad (4)$$

Table 7 shows the ANOVA for the roughness (Ra), the feed rate f (mm/rev) has the greatest influence on Ra with a contribution of 82.35%, followed by the factor Vc (m/min) with a contribution of 9.48%. The other factors (Doc and cutting tool material) are not significant, with contributions of 4.45% and 2.14%, respectively. Similarly, De Souza et al. [38] and Zerti et al. [39] found similar results when turning AISI 52100 and AISI 420 hardened steels using TiN-coated inserts, respectively. Finally, the feed rate (f) must be carefully controlled and maintained within an optimum range to minimize surface roughness during machining operations, thus guaranteeing better-quality machined surfaces.

Since some factors are not significant, the model is updated using the pooling technique, removing the non-significant independent variable, as explained in the work of [40,41]. The elimination of factors occurs in the following order: (1) cutting tool material (Ti), followed by (2) depth of cut (Doc). Table 8 shows the ANOVA of Ra after pooling Ti, where the factors Vc and f are significant ($p<0.05$). However, the Doc factor remains insignificant with $p=0.059$. Table 9 shows the ANOVA for Ra after pooling Doc; the factors Vc and f are the only independent variables explored that have a significant influence on Ra, resulting in the following model:

$$VB_{(T2)} = -0.216 + 0.001171 \times Vc + 6.9 \times f \,. \quad (5)$$

Main effects graphs have been drawn up to illustrate the influence of cutting factors on output parameters (Figure 2). The curve with the highest slope indicates the factor with the

greatest impact on the parameter studied. The f(mm/rev) factor has a strong influence on Ra, while the Vc factor has a significant effect on VB.

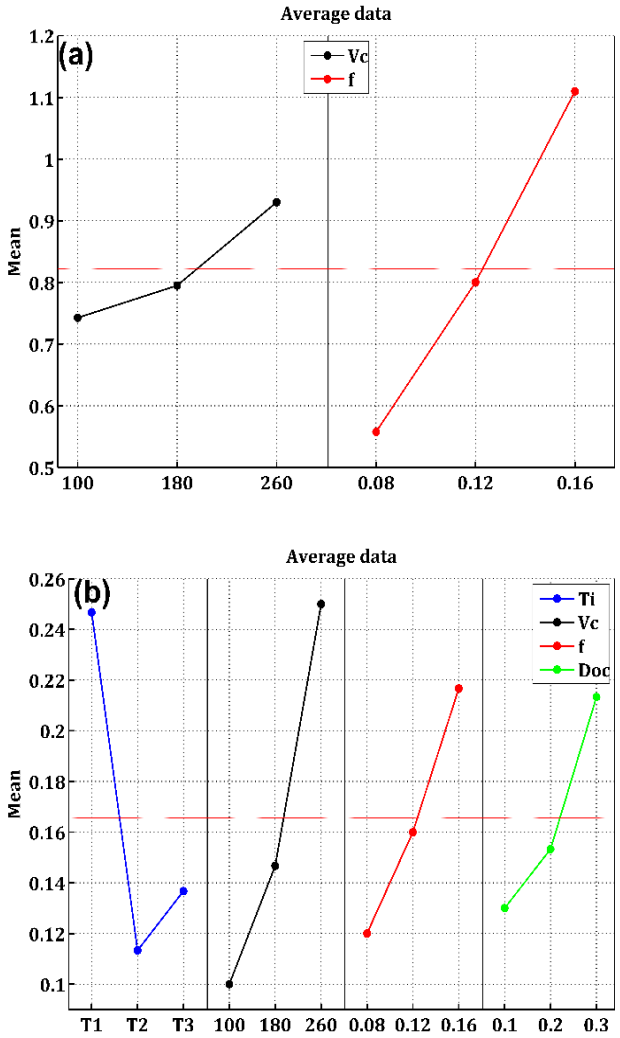


**Fig. 2**. Main effects graph for (a): Ra, (b):VB.

Figure 2-a shows that Ra increases with increasing f (mm/rev) and Vc (m/min). This phenomenon is explained by the movement of the tool and the workpiece, which generates helical grooves on the machined surface. As the cutting parameters are increased, these grooves become deeper and wider. Similar results were reported by Safi et al. [17] in their study of tool wear and the evolution of 3D surface topography as a function of cutting parameters when turning X210Cr12 steel with coated carbide tools ($Al_2O_3$/TiC/TiCN). Furthermore, Ra decreases with increasing Doc.

In terms of the influence of the cutting tool material, the T2 insert achieved the best roughness thanks to its TiN coating, which improves wear resistance. It was followed by the T3 insert, then the T1 insert, whose roughness was more affected by tool wear and breakage.

Figure 2-b shows a significant increase in VB wear as Vc rises, followed by f and then Doc. A high value of cutting speed significantly influenced the occurrence of tool wear and the formation of chips due to the generation of excessive heat, in addition to workpiece wobbling, vibration, and chattering [42]. The T2 insert experiences minimal wear, followed by the T3 insert, and then the T1 insert, which is rumpled in Test No3.

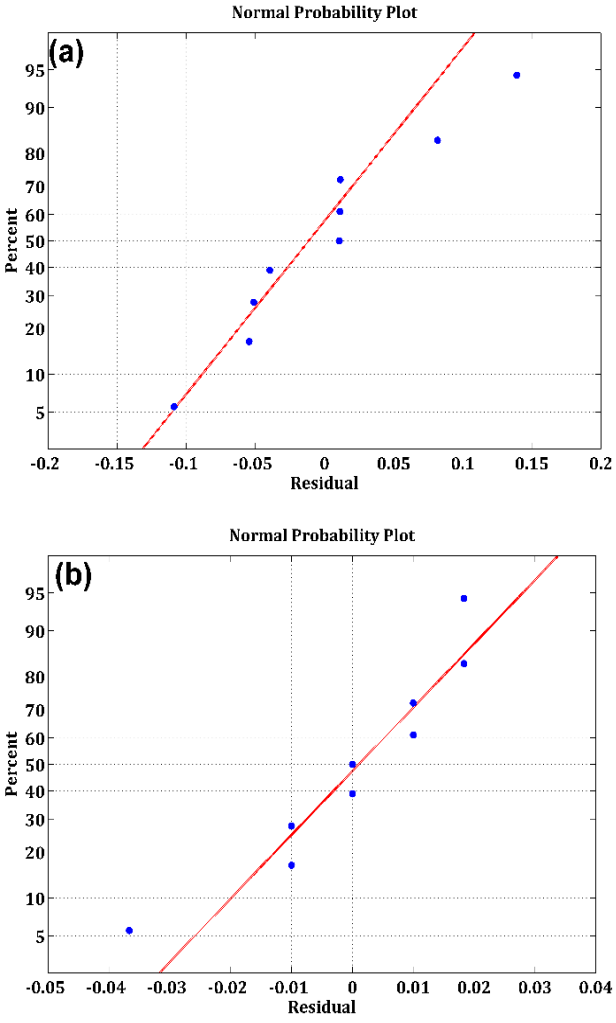


**Fig. 3**. Normal plots for residuals (a): Ra, (b):VB.

Figure 3(a)-(b) displays the normal probability curves for the residuals of the output parameters (Ra and VB) from the ANOVA analysis. These plots allow us to assess the normality of the residuals and, consequently, the validity of the ANOVA assumptions.

Examination of the graphs shows that, overall, the residuals follow a trend close to the reference line at 45°, indicating an approximately normal distribution with relatively little dispersion. This suggests that the assumption of normality of the residuals is reasonably respected, reinforcing the validity of the results of the analysis. The model is therefore statistically valid.

### 3.2 Analysis of tool wear VB

Figures 4, 5 and 6 show the flank wear (VB) for the three cutting inserts CC650, CC6050 and CC670, respectively. The results indicate that the wear of all three inserts remained within the allowable limit specified by the ISO 3685 standard (VB=0.3 mm) [17], except in the case of test 3 with the T1 insert (CC650), where Vc, f and Doc were maximum and showed the highest wear with VB=0.43 mm. The T2 cutting insert (CC6050) had the lowest wear with VB =0.09 mm, followed by the T3 insert (CC670) with VB=0.18 mm. This difference is mainly due to the physical and mechanical properties of the three inserts used, as well as the presence of the TiN coating in the CC6050 cutting insert, which reduces the abrasive wear. Saikaew et al. [42] obtained comparable results to ours regarding the machining performance of $Al_2O_3$+TiC inserts for dry turning of AISI 4140 steel.

Figure 4 shows the wear on the T1 insert in tests 1, 2 and 3. For tests 1 and 2, wear appears in the form of a striated band, indicating an abrasive wear mechanism.

This phenomenon is caused by the friction of hard particles on the cutting edge, leading to progressive abrasion of the tool. With test 3, the cutting conditions are at their highest (Vc=260 m/min, f=0.16 mm/rev and Doc=0.3 mm); micro-chips accumulating on the cutting edge increase the wear rate, leading to localized chipping and fracture on the tool nose. A higher cutting speed generates more friction and heat at the tool-chip interface, leading to the softening of the tool material. This accelerates the chipping process at the cutting edge, also due to the increased abrasive action of the workpiece particles and the microchips cumulated there [43]. Using SEM (Figure 7) on the cutting surface of the CC650 insert, chipping and breakage of the cutting edge were observed. This clearly demonstrates that the uncoated T1 insert (CC650) is not recommended for machining this material under severe machining conditions. Its brittleness and sensitivity to impact are the main causes of its damage. Marigoudar et al. [44] observed a fracture at the tip of an uncoated ceramic tool with a higher Ra roughness.

Figure 5 shows the wear morphology of the T2 insert (CC6050) during trials 4, 5 and 6. The wear recorded is at its minimum level and without the presence of chipping on the cutting edges in all the tests, in particular for test 4, where the lowest wear of the nine tests was measured to be VB=0.09 mm, followed by test 5 to VB=0.11 mm. The maximum wear measured with this insert is VB=0.14 mm at test 6 (Vc=260 m/min, f=0.08 mm/rev and Doc=0.2 mm), which is due to the accumulation of chips near the cutting edge, indicating interaction with the machined material and contributing to adhesive wear. The presence of the TiN coating in this insert provides toughness and strength to the tool, minimizing the progression of abrasive wear [45]. These results are in good agreement with those presented in the works of Lungu et al. [46] and Zheng et al. [47].

Figure 6 shows the wear on the T3:CC670 insert obtained in tests 7, 8 and 9. The wear is in the range VB= [0.11-0.18] mm. An abrasive wear mechanism developed during the three tests via the striations observed on the surfaces of the cutting inserts. The cause is due to the increase in cutting temperature caused by the increase in Vc and the hardness of the workpiece. Wear is greater than on the T2:CC6050 insert and increases as Vc increases. Traces of chipping were present on the cutting edge during test 9 (Vc=260 m/min, f=0.12 mm/rev and Doc=0.2 mm) caused by the accumulation of chips, the increase in temperature near the cutting edge, and the brittleness of the tool material [48].

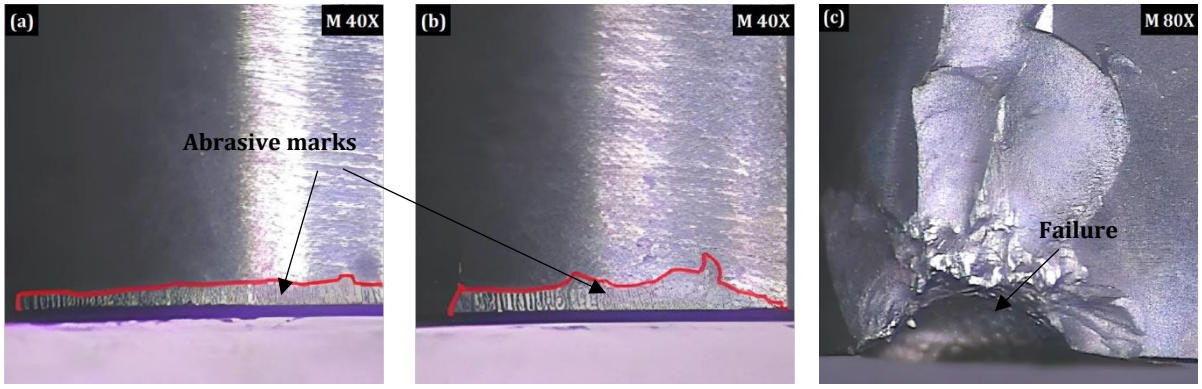


**Fig. 4.** Flank wear of T1 insert, (a): Vc=100 m/min, f=0.08 mm/rev, Doc,0.1 mm; (b):Vc=180 m/min, f=0.12 mm/rev, Doc=0.2 mm; (c):Vc=260 m/min, f=0.16 mm/tr, Doc=0.3mm.

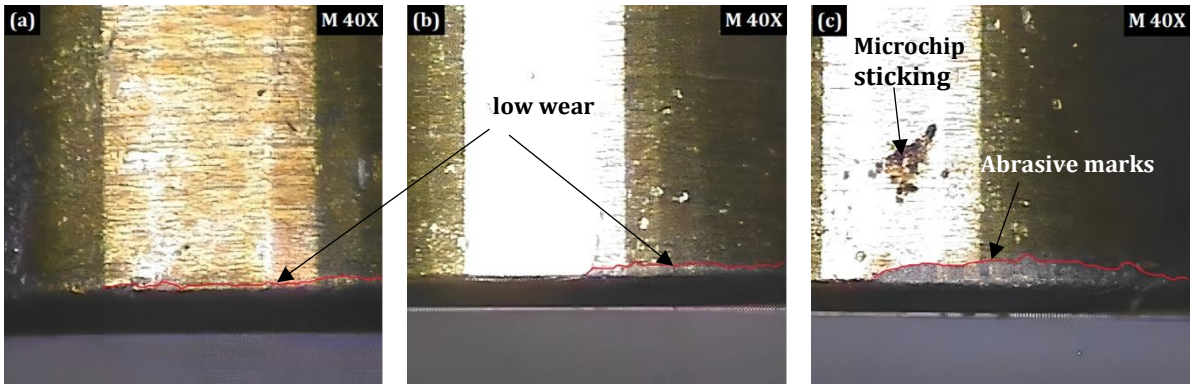


**Fig. 5.** Flank wear of T2 insert, (a): Vc=100 m/min, f=0.08 mm/rev, Doc,0.1 mm; (b):Vc=180 m/min, f=0.12 mm/rev, Doc=0.2 mm; (c):Vc=260 m/min, f=0.16 mm/tr, Doc=0.3mm.

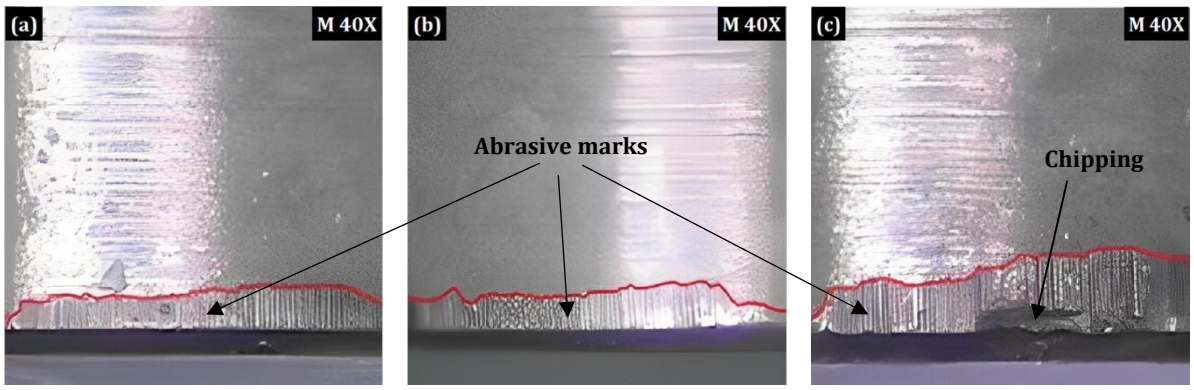


**Fig. 6.** Flank wear of T3, (a): Vc=100 m/min, f=0.08 mm/rev, Doc,0.1 mm; (b):Vc=180 m/min, f=0.12 mm/rev, Doc=0.2 mm; (c):Vc=260 m/min, f=0.16 mm/tr, Doc=0.3mm.

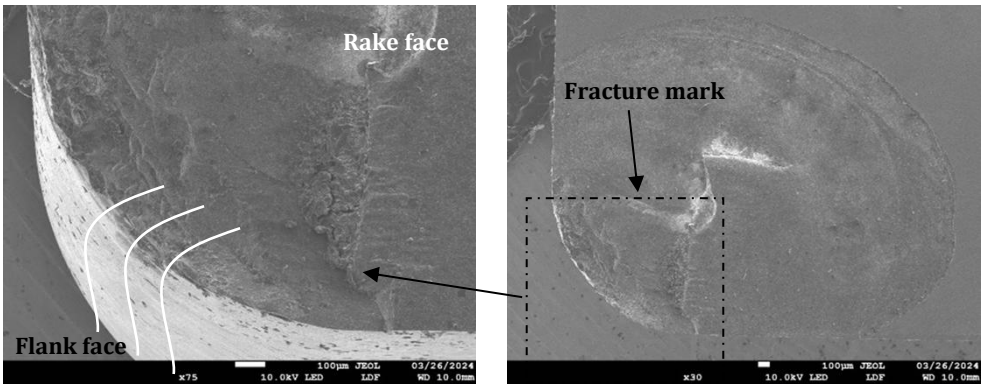


**Fig. 7.** SEM image of cutting edge T1 at Vc=260 m/min, f=0.16 mm/rev and Doc=0.3 mm.

## 4. OPTIMIZATION

### 4.1 Mono-objective-optimization

The Taguchi method is a powerful design approach for improving and optimizing industrial production [49,50]. This method transforms the output parameters, such as Ra, VB, and MRR, into the signal-to-noise ratio (S/N) [51,52]. For the minimization case, equation (6) was used to determine the S/N of Ra and VB, while equation (7) was used to calculate the S/N of MRR for the maximization case.

Table 10 presents the elements of the decision matrix, defined by the S/N ratios of the technological parameters (Ra, VB, and MRR).

$$S/N_{Ra,VB} = -10 \times \log\left(\frac{1}{N}\sum_{i=1}^{n} y_i^2\right) \quad (6)$$

$$S/N_{MRR} = -10 \times \log\left(\frac{1}{N}\sum_{i=1}^{n} \frac{1}{y_i^2}\right) \quad (7)$$

**Table 10.** S/N values for output parameters Ra, VB and MRR.

| Tests | Input parameters | | | | Output parameters | | |
|---|---|---|---|---|---|---|---|
| | Ti | Vc | f | Doc | S/N (Ra) | S/N (VB) | S/N (MRR) |
| 1 | T1 | 100 | 0.08 | 0.1 | 4.55357 | 20 | 58.0618 |
| 2 | T1 | 180 | 0.12 | 0.2 | 2.12476 | 13.5556 | 72.7097 |
| 3 | T1 | 260 | 0.16 | 0.3 | -1.60531 | 7.3306 | 81.9243 |
| 4 | T2 | 100 | 0.12 | 0.2 | 4.15217 | 20.9151 | 71.1261 |
| 5 | T2 | 180 | 0.16 | 0.3 | -0.90646 | 19.1721 | 69.1878 |
| 6 | T2 | 260 | 0.08 | 0.1 | 4.59769 | 17.0774 | 72.3819 |
| 7 | T3 | 100 | 0.16 | 0.3 | -0.13787 | 19.1721 | 70.1030 |
| 8 | T3 | 180 | 0.08 | 0.1 | 6.16070 | 18.4164 | 72.7097 |
| 9 | T3 | 260 | 0.12 | 0.2 | 0.01739 | 14.8945 | 69.8831 |

#### 4.1.1 Optimization of Ra

Table 11 shows the average signal-to-noise ratio (S/N) values of Ra for each level of input parameters. It is clear that the most influential factor on Ra is the feed rate (f), with an effect of 5.9872, followed by the cutting speed (Vc) with an effect of 1.8527, and then the depth of cut (Doc) with an effect of 1.681. On the other hand, the cutting material exerted a relatively weak influence, with an effect of 0.9235. It should be noted that the higher the delta value, the more significant the impact of the control factor.

**Table 11.** S/N responses for Ra.

| Level | 1 | 2 | 3 | Delta | Rang |
|---|---|---|---|---|---|
| Ti | 1.691 | 2.6145 | 2.0134 | 0.9235 | 4 |
| Vc | 2.856 | 2.4596 | 1.0033 | 1.8527 | 2 |
| f | 5.104 | 2.0981 | -0.8832 | 5.9872 | 1 |
| Doc | 1.2215 | 2.1949 | 2.9025 | 1.681 | 3 |

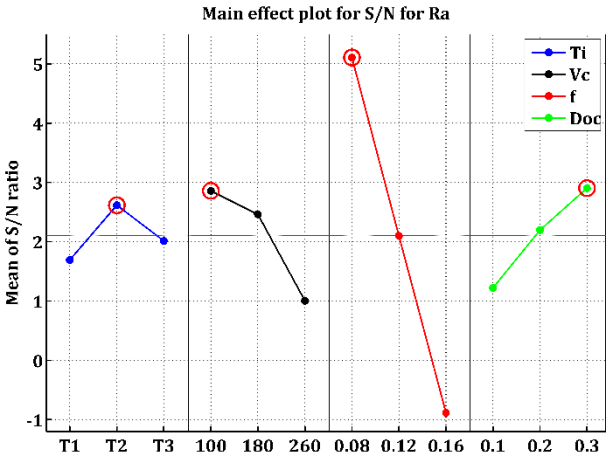


**Fig. 8.** Main effect plot for S/N for Ra.

According to Taguchi's method, the maximum value of S/N indicates the best performance in terms of Ra response. Figure 8 illustrates that the optimum combination of input parameters for minimizing Ra is (T1, Vc1, f1, and Doc3), corresponding to the configuration (Vc = 100 m/min; f = 0.08 mm/rev; Doc = 0.3 mm) with the CC6050 cutting insert, which suggests that lower speeds and lower feeds minimize Ra as reported

in the works of Thabane et al. [43]. This finding contradicts some earlier observations where Ra decreased at higher speeds from 200 m/min to 1200 m/min [53].

### 4.1.2 Optimization of VB

Table 12 illustrates the influence of turning process parameters on the signal-to-noise ratio (S/N) of VB. Among these parameters, the Vc factor and the cutting material are found to be the most significant determinants of VB, while the feed rate (f) and the depth of cut (Doc) have a less significant impact. The optimum cutting parameters identified were T2, Vc1, f1, and Doc1, corresponding to the CC6050 insert, with values of Vc=100 m/min, f=0.08 mm/rev, and Doc=0.1 mm. These results were confirmed by the S/N ratio main effect diagram for VB, shown in Figure 9.

**Table 12.** S/N responses for VB.

| Level | 1 | 2 | 3 | Delta | Rang |
|---|---|---|---|---|---|
| Ti | 13.63 | 19.05 | 17.49 | 5.43 | 2 |
| Vc | 20.03 | 17.05 | 13.1 | 6.93 | 1 |
| f | 18.5 | 16.46 | 15.22 | 3.27 | 3 |
| Doc | 18.02 | 16.6 | 15.55 | 2.47 | 4 |

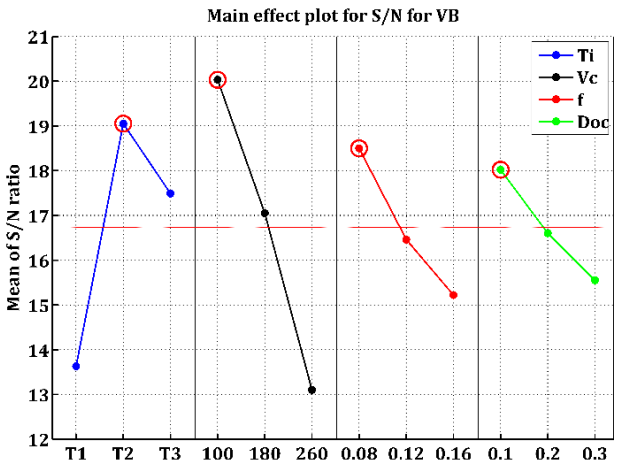


**Fig. 9.** Main effect plot for S/N for VB.

This analysis shows that Vc is the most influential control factor on the wear VB (Delta=6.93), followed by the cutting material (Delta= 5.43). On the other hand, the factors f and Doc have less significant influences with values of 3.27 and 2.47, respectively.

Figure 9 shows that VB increases rapidly as Vc and f increase and more moderately as Doc increases. Furthermore, this figure reveals that the average S/N varies considerably between levels 1 and 2 of the cutting material, with an advantage for the T2:CC6050 insert.

### 4.1.3 Optimization of MRR

Table 13 shows the single-objective optimization of the material removal rate (MRR). It is clear that this variable reaches its maximum when the levels of Vc, f, and Doc are at their maximum value (Vc3, f3, Doc3). The material of the cutting tool is not a decisive factor in the material removal rate (MRR) with a Delta value of zero. Increasing Vc, f, and Doc leads to an increase in MRR, as shown in Figure 10.

**Table 13.** S/N responses for MRR.

| Level | 1 | 2 | 3 | Delta | Rang |
|---|---|---|---|---|---|
| Ti | 70.9 | 70.9 | 70.9 | 0 | 4 |
| Vc | 66.43 | 71.54 | 74.73 | 8.3 | 2 |
| f | 67.72 | 71.24 | 73.74 | 6.02 | 3 |
| Doc | 65.71 | 71.73 | 75.25 | 9.54 | 1 |

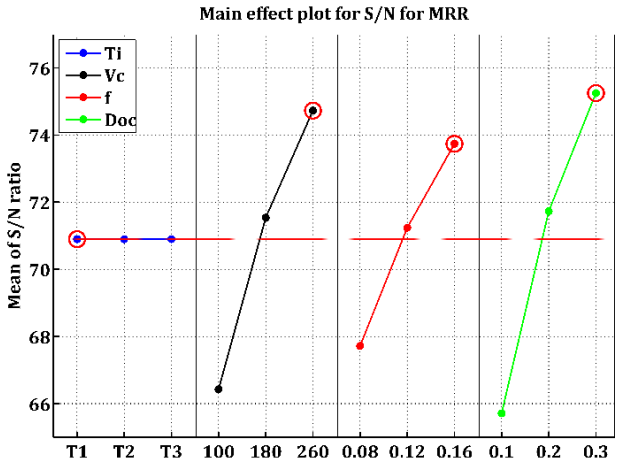


**Fig. 10.** Main effect plot for S/N for MRR.

The most significant impact appears to be that of the Doc depth of cut, followed by the cutting speed (Vc) and the feed rate (f). The regimes obtained are comparable to those found in studies of Sathiya et al. [54] and Abdullahu et al. [55], which show that increasing the cutting speed also leads to an increase in the distance between the cutting tool and the workpiece. As the parameter f increases, the proximity between the cutting tool edge and the workpiece increases rapidly, while an increase in the parameter (Doc) leads to an increase in the perpendicular distance between the machined surface and the unmachined work surface.

### 4.2 Multi-objective optimization MCDM

Optimization methods are powerful techniques that can improve the execution of processes in industry and make it possible to link technical and economic approaches [56,57]. This optimization makes it possible to find a compromise between the three output parameters Ra, VB and MRR, offering a more balanced approach compared with single-objective optimization, which treats each parameter separately [58]. This section implements two methods, GRA and DEAR, to optimize the hard turning process of AISI 4140 steel. These methods were chosen because of their effectiveness in optimizing machining processes in particular and their wide applications in various scientific fields [55,59].

Sometimes, certain attributes are more important than others; in this study, the technological parameters are equally important.

The first step in these approaches is to generate a decision matrix of the problem ($x_{ij}$) using equation (8), where the different objectives Ra, VB, and MRR are converted into S/N to determine the input parameters for the approaches, as shown previously in Table 10.

$$\left(x_{ij}\right)_{k\times n}=\begin{bmatrix} x_{11} & x_{1j} & \cdots & x_{1n} \\ x_{in} & x_{ij} & \cdots & x_{in} \\ \cdots & \cdots & \cdots & \cdots \\ x_{k1} & x_{kj} & \cdots & x_{kn} \end{bmatrix} \tag{8}$$

Where $x_{ij}$ indicates the element of the decision matrix for the $i^{th}$ alternative in the $j^{th}$ attribute, with i= 1, 2, ..., k = 16 and j = 1, 2, n = 3).

#### 4.2.1 GRA Method

Grey relational analysis is a multiple response optimization technique that identifies an appropriate solution to complex real-world problems. The following steps are generally considered for grey relational analysis [60].

**Step 1**: The GRA method is based on the normalization of the decision element of the matrix ($x_{ij}$) using equation (9).

$$G_x(p)=\frac{x_{ip}-\min(x_{ip})}{\max(x_{ip})-\min(x_{ip})} \tag{9}$$

Where Gi(p) represents the normalized value of $x_{ip}$, while max($x_{ip}$) and min($x_{ip}$) correspond respectively to the maximum and minimum values of xip for i varying from 1 to k = 9. For our analysis, we decided to examine the signal-to-noise ratio (SNR) values for the different parameters under study, namely Ra, VB and MRR. Optimal performance is achieved with a maximum value of signal-to-noise ratio (S/N), which justifies the use of equation (5) for normalization.

**Step 2:** Equations (10) to (13) are used to determine the grey relational coefficient ($\varphi_i(p)$), which reflects the correlation between the results obtained by calculation and those obtained from experiments.

$$\varphi_i(p)=\frac{\Delta_{\min}+\xi\Delta_{\max}}{\Delta_{oi}(p)+\xi\Delta_{\max}} \tag{10}$$

In this study, the coefficient of distinction ($\xi$) was set at 0.5 in order to adjust the relational coefficient. $\Delta_{oi}(p)$ represents the difference in absolute value between the ideal value $G_0(p)$ and the value $G_i(p)$.

$$\Delta_{0i}(p)=\left\|G_0(p)-G_i(p)\right\| \tag{11}$$

$$\Delta_{\min}=\min_{\forall i}\min_{\forall p}\left\|G_0(p)-G_i(p)\right\| \tag{12}$$

$$\Delta_{\max}=\max_{\forall i}\max_{\forall p}\left\|G_0(p)-G_i(p)\right\| \tag{13}$$

**Step 3**: Equation (14) is used to calculate the grey relationship gradient ($\delta_i$) from the results φi (p) in order to express the level of correlation between the series; the calculated results are presented in Table 14.

$$\delta_i=\frac{1}{n}\sum_{p=1}^{n}\left[\varphi_i(p)\right] \tag{14}$$

Where n is the number of process response parameters.

In the GRA method [60], the largest value of $\delta_i$ is taken as the strongest relationship between the ideal sequence $G_0(P)$ and the experimental sequence $G_i$ (P). The multi-objective optimization is converted to a single-objective optimization when δi is calculated.

**Table 14.** GRA results.

| Tests | Normalization $G_0(P)$ | | | GRC φi (p) | | | GRC $\delta_i$ | S/N (CRG) |
|---|---|---|---|---|---|---|---|---|
| | Ra | VB | MRR | Ra | VB | MRR | | |
| 1 | 0.793 | 0.933 | 0 | 0.707 | 0.881 | 0.333 | 0.641 | -5.863 |
| 2 | 0.480 | 0.458 | 0.614 | 0.490 | 0.480 | 0.564 | 0.512 | -5.815 |
| 3 | 0 | 0 | 1 | 0.333 | 0.333 | 1 | 0.556 | -5.099 |
| 4 | 0.741 | 1 | 0.547 | 0.659 | 1 | 0.525 | 0.728 | -2.757 |
| 5 | 0.090 | 0.872 | 0.466 | 0.355 | 0.796 | 0.484 | 0.545 | -5.272 |
| 6 | 0.799 | 0.717 | 0.6 | 0.713 | 0.639 | 0.556 | 0.636 | -3.931 |
| 7 | 0.189 | 0.872 | 0.505 | 0.381 | 0.796 | 0.502 | 0.560 | -5.036 |
| 8 | 1 | 0.816 | 0.614 | 1 | 0.731 | 0.564 | 0.765 | -2.327 |
| 9 | 0.209 | 0.557 | 0.495 | 0.387 | 0.530 | 0.498 | 0.472 | -6.521 |

**Table 15.** S/N responses for $\delta_i$.

| Factor | Level 1 | Level 2 | Level 3 |
|---|---|---|---|
| **Ti** | -4.925 | -3.987 | -4.628 |
| **Vc** | -3.885 | -4.4471 | -5.184 |
| **f** | -3.373 | -5.031 | -5.136 |
| **Doc** | -5.219 | -4.927 | -3.394 |
| **Optimal regime** | T2, Vc1, f1, Doc3 | | |

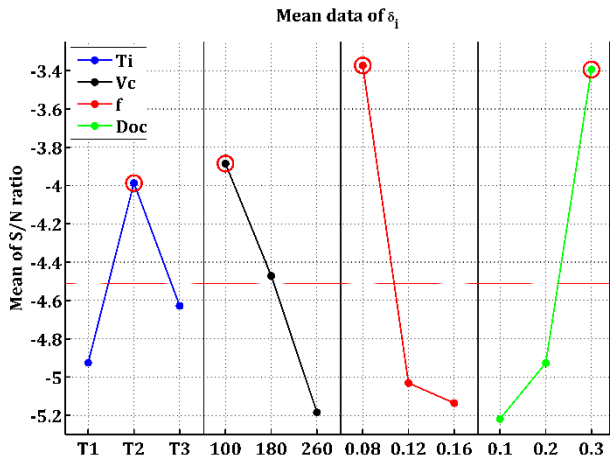


**Fig. 11.** Main effect plot for S/N for GRA method.

The main effects diagram of the average S/N values of $\delta_i$ is used to determine the combination of optimum levels (Figure 11). Table 15 shows the average S/N of $\delta_i$ at each level of machining parameters. The ideal level of cutting conditions is the one corresponding to the largest value of S/N ($\delta_i$). Thus, it can be deduced from Figure 11 and Table 13 that the optimum combination corresponds to T2, Vc1, f1, and Doc3; in other words, simultaneous optimization of Ra, VB, and MRR leads to Vc = 100 m/min, f = 0.08 mm/rev, and Doc = 0.3 mm with the CC6050 insert.

### 4.2.2 DEAR Method

The DEAR method has advantages over other statistical optimization methods in that it does not require a fraction of a weight to be assigned to each result. In the analysis, the initial measured responses are assigned a value that can be treated as a Multi-Criteria Performance Index (MCPI) value in order to find the optimal combination of process parameters. It uses the following sequential steps:

**Step 1**: Calculation of the weighting of each response ($W_{Ra}$, $W_{VB}$ and $W_{MRR}$).

The weight corresponds to the ratio of the response to the sum of the responses as described in equations (15), (16) and (17).

$$W_{Ra} = \frac{Ra}{\sum Ra} \tag{15}$$

$$W_{VB} = \frac{VB}{\sum VB} \tag{16}$$

$$W_{MRR} = \frac{MRR}{\sum MRR} \tag{17}$$

**Step 2:** Convert the response data into weight data by multiplying the response data by their own weights as described in Equations (18), (19) and (20).

$$A = W_{Ra} \times Ra \tag{18}$$

$$B = W_{VB} \times VB \quad (19)$$

$$C = W_{MRR} \times MRR \quad (20)$$

Step 3: Calculation of the MRPI index using equation (21).

$$MRPI_i = A + B + C \quad (21)$$

The calculated weighting values and MRPI values for each experiment are shown in Table 16.

**Table 16.** Optimization results based on DEAR method.

| Tests | W(Ra) | W(VB) | W(MRR) | MRPI | MRPI (S/N) |
|---|---|---|---|---|---|
| **1** | 0.240 | 0.133 | 0.091 | 9.034 | 19.118 |
| **2** | 0.112 | 0.09 | 0.114 | 9.744 | 19.775 |
| **3** | -0.085 | 0.049 | 0.128 | 11.011 | 20.837 |
| **4** | 0.219 | 0.139 | 0.111 | 11.744 | 21.396 |
| **5** | -0.049 | 0.127 | 0.108 | 9.987 | 19.989 |
| **6** | 0.243 | 0.113 | 0.113 | 11.263 | 21.033 |
| **7** | -0.007 | 0.127 | 0.109 | 10.145 | 20.125 |
| **8** | 0.325 | 0.122 | 0.114 | 10.54 | 21.966 |
| **9** | 0.001 | 0.099 | 0.11 | 9.127 | 19.207 |

The main effects diagram of the average S/N values of MRPI is used to determine the combination of optimal levels (figure 12). Table 17 shows the average S/N ratio of MRPI at each level of the machining parameters. The ideal level of cutting conditions is the one that corresponds to the highest value of S/N (MRPI). Thus, we can deduce from Figure 12 and Table 15 that the optimal combination corresponds to T2, Vc2, f1, and Doc3; in other words, the simultaneous optimization of Ra, VB, and MRR leads to the regime Vc = 180 m/min, f = 0.08 mm/rev, and Doc = 0.3 mm with the CC6050 insert.

**Table 17.** S/N responses for MRPI.

| Factor | Level 1 | Level 2 | Level 3 |
|---|---|---|---|
| **Ti** | 19.91 | 20.81 | 20.43 |
| **Vc** | 20.21 | 20.58 | 20.36 |
| **f** | 20.71 | 20.13 | 20.32 |
| **Doc** | 19.44 | 20.31 | 21.40 |
| **Optimal regime** | T2, Vc2, f1, Doc3 | | |

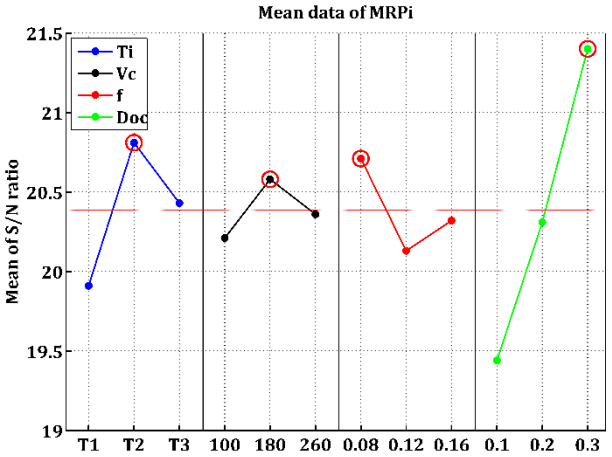


**Fig. 12.** Main effect plot for S/N of DEAR method.

### 4.2.3 Finding and comparison between the approaches

The optimal cutting regimes found for the performance parameters (Ra, VB, and MRR) are not included in the $L_9$ experimental plan adopted in this study. Consequently, Equation (22) [60] was used to determine the S/N prediction values of the results (Ra et VB and MRR).

$$\bar{\varphi} = \varphi_m + \sum_{i=1}^{q} (\bar{\varphi}_i - \varphi_m) \quad (22)$$

With:

$\bar{\varphi}$: Accepted value of the responses under optimal conditions.

$\varphi_m$: Average of all the S/N ratios for each response.

$\bar{\varphi}_i$: Average of the S/N ratios that correspond to the optimal level of each input parameter.

*q:* Number of each parameter.

Then equations (23) and (24) are used to convert the predicted values of the S/N ratio calculated by equation (18) to the actual values for the parameters Ra, VB, and MRR [60]:

Minimization:

$$\text{Real values } (Ra, VB) = \sqrt{10^{(\frac{-\bar{\varphi}}{10})}} \quad (23)$$

$$\text{Real values (MRR)} = \frac{1}{\sqrt{10^{(\frac{-\bar{\varphi}}{10})}}} \quad (24)$$

Table 18 summarizes the optimal regimes obtained with the two optimization methods used and the corresponding responses Ra, VB,

and MRR. It can be seen that for both the DEAR and GRA methods, the optimization results maintain the same feed rate (f = 0.08 mm/rev), depth of cut (Doc = 0.3 mm), and cutting insert (T2/CC6050) with the exception of the cutting speed Vc, which is equal to 100 m/min for the GRA method. This value corresponds to a minimum roughness Ra (Ra=0.439 µm) and low wear (VB=0.071 mm). For the DEAR method, a cutting speed of 180 m/min helped to raise the material removal rate to MRR = 4320 $mm^3$/min and slightly raise wear to 0.1 mm and roughness to Ra 0.459 µm.

**Table 18.** Optimal regimes and responses.

| Methods | Optimal regime | Responses | | |
|---|---|---|---|---|
| | | Ra (µm) | VB (mm) | MRR ($mm^3$/min) |
| GRA | T2, Vc1, f1, Doc3 | 0.439 | 0.071 | 2400 |
| DEAR | T2, Vc2, f1, Doc3 | 0.0459 | 0.1 | 4320 |

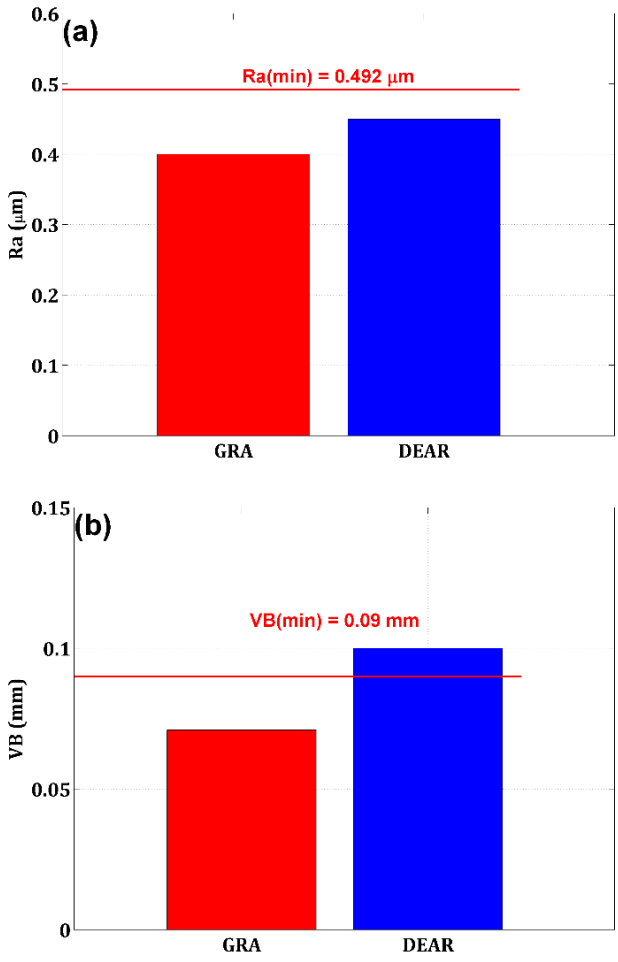


**Fig. 13.** Optimization results using GRA and DEAR methods.

Figure 13 shows a comparison of these responses (Ra and VB). The red horizontal line shows the minimum values for Ra and VB, which correspond to the experimental results of Taguchi $L_9$ (Table 5). We observe that the optimal regimes produce Ra and VB values below or close to their minimum levels.

### 4.3 Confirmation tests

Experimental validation tests were carried out on the accuracy of the optimal regimes exposed in Table 16. The calculation of the percentage error is performed using equation (25) [61].

$$P_e = \frac{\left|Y_{\exp} - Y_{prd}\right|}{Y_{\exp}} \times 100 \quad (25)$$

Where:
$Y_{exp}$: Experimental value
$Y_{prd}$: *Predicted* value
$P_e$: Error percentage

The confirmatory tests were planned and performed based on the optimal levels of the optimal cutting parameters obtained by the two methods, GRA and DEAR, for the machining of AISI 4140. Table 19 illustrates the results of confirmation tests as well as the predicted values of Ra and VB and the errors found. It can be seen that the relative error is 1.85% for the GRA method and 2.45% for the DEAR method in the case of Ra and 4.05% for the GRA method and 4.76% for the DEAR method in the case of VB. It can be seen that the maximum error reaches 4.76% which confirms the validity of the optimal results obtained in this study. This percentage of error can be attributed to other uncontrollable factors such as machine vibration, climatic conditions, and human error.

The confidence interval (CI) is used to estimate a population parameter by defining a range within which this parameter has a certain probability of occurring. The shorter the interval, the more precise the estimate. Since it is difficult to analyze the entire population, a sample is used to calculate a point estimate and a confidence interval, thus guaranteeing a high probability that the parameters considered accurately reflect those of the population.

In the confirmation tests, the confidence interval is determined from the estimate of the mean of the final output parameters, obtained from the optimal results (T2, Vc1, f1 and Doc3) for GRA and (T2, Vc2, f1 and Doc3) for DEAR, according to Table 19.

**Table 19. Confirmation tests.**

| | Ti | Vc | f | Doc | Ra | | | VB | | |
|---|---|---|---|---|---|---|---|---|---|---|
| | | | | | Experiment | Prediction | Error [%] | Experiment | Prediction | Error [%] |
| **GRA** | T2 | 100 | 0.08 | 0.3 | 0.431 | 0.439 | 1.85 | 0.074 | 0.071 | 4.05 |
| **DEAR** | T2 | 180 | 0.08 | 0.3 | 0.448 | 0.459 | 2.45 | 0.105 | 0.1 | 4.76 |

A confidence interval (CI) for predicting the mean of Ra and VB [62-64] based on the confirmation experiment is calculated as equation (26):

$$CI = \sqrt{F_{0.05}(3, f_e)Ve\left[\frac{1}{n}+\frac{1}{R}\right]} \quad (26)$$

Where:

$f_e$: Error degree of freedom from Tables (6 and 9), 3 for VB and 6 for Ra

$F_{0.05}(3, fe)$: Fraction taken from standard "F" table.

$F_{0.05}$ (3,3) =9.28 for VB and $F_{0.05}$ (3,6) =4.76 for Ra.

*Ve*: Error variance (0.0008 for VB and 0.007572 for Ra) taken from the ANOVA Tables (6 and 9).

*R*=1: Number of replicants of the confirmation experiment.

n=9/ (1+8) =1: Effective No. of replicants.
The 95% CI of the optimal Ra and VB based on the confirmation experiment is expressed by equations 27 and 28:

$$(Ra_{em} - CI) < \mathrm{Ra}_{con} < (Ra_{em} + CI) \quad (27)$$

$$(\mathrm{VB}_{em} - CI) < VB_{con} < (\mathrm{VB}_{em} + CI) \quad (28)$$

From the above relation, the values of the confidence interval (CI) for Ra and VB are CI(Ra)=0.268 and CI(VB)=0.122.

Where $Ra_{em}$ and $VB_{em}$ are the predicted values of Ra and VB given in Table 19**.** The results obtained from the confirmation experiments prove that the determined Ra and VB lie inside the confidence interval.

(i.e., 0.431 falls between 0.171 and 0.707)
(i.e., 0.074 falls between -0.051 and 0.193)
(i.e., 0.448 falls between 0.191 and 0.727)
(i.e., 0.105 falls between -0.022 and 0.222)

## 5. CONCLUSION

This study focused on the multi-objective optimization of the cutting conditions (Vc, f, and Doc) and tool material during the hard machining of AISI 4140 steel using Taguchi-based GRA and DEAR methods. The objective was to achieve a balance between the three output parameters (VB, Ra, and MRR). Based on the experimental results and optimization analysis, the following conclusions were drawn:

1. The lowest tool wear (VB = 0.09 mm) was observed in Test No. 4 (T2, Vc=100m/min, f=0.12mm/tr Doc=0.3 mm), while the highest wear (VB= 0.43 mm) occurred in Test No. 3 (T1, Vc = 260 m/min, f = 0.16 mm/rev, Doc = 0.3 mm) attributed to tool edge breakage.
2. Feed rate (f) has the greatest impact on Ra (82.35% contribution); while cutting speed (Vc) and feed rate (f) are the most influential on VB, contributing 37.03% and 35.46%, respectively.
3. Among the tested tools, the TiN-coated ceramics insert (CC6050) exhibited superior performance in terms of surface finish and wear resistance.
4. The Taguchi-GRA-DEAR approach proved effective for multi-objective optimization in hard machining, avoiding the need for complex mathematical models.
5. The GRA method identified the optimal regime (T2, Vc1, f1, Doc3) for minimizing Ra and VB, while the DEAR method suggested a slightly different regime with Vc2 to enhance productivity.

6. The confirmatory tests validated the optimization, showing a maximum error of only 4.76% compared to the predictions, which confirms the reliability of the optimal results. Moreover, the experimental results falling within the confidence interval reinforcing the overall validity of the obtained results.

## FUTUR SCOPE

As part of future research, several lines of investigation could be envisaged. A first approach would be to explore the use of other tool materials, such as CBN and cermet, to improve wear resistance. Furthermore, the integration of additional input parameters, such as the radius of the cutting tool, as well as output parameters such as vibration and cutting force, could enable a more detailed analysis of the machining process. Another promising approach would be the application of advanced optimization techniques, including hybrid artificial intelligence, to refine predictive models.
Finally, the study of lubrication and cooling strategies, in particular using ML and NMQL techniques, can help to extend tool life and improve overall process performance.

## Acknowledgement

This research was undertaken by the Laboratory of Mechanics, Materials and Energy at the University of Bejaia in collaboration with the Laboratory of Mechanics and Structure (LMS) at the University 8 Mai in Guelma, Algeria.

## REFERENCES

[1] R. Mallick, R. Kumar, A. Panda, and A. K. Sahoo, "Hard Turning Performance Investigation of AISI D2 Steel under a Dual Nozzle MQL Environment," *Lubricants*, vol. 11, no. 1, p. 16, Jan. 2023, doi: 10.3390/lubricants11010016.

[2] V. F. C. Sousa and F. J. G. Silva, "Recent Advances in Turning Processes Using Coated Tools—A Comprehensive Review," *Metals*, vol. 10, no. 2, p. 170, Jan. 2020, doi: 10.3390/met10020170.

[3] S. W. H. Zubair, S. M. Arafat, S. A. Khan, G. M. Uddin, and N. Hayat, "Dry finishing turning of AA7075 with binary and ternary nitrides and carbides ceramic-coated tools," *The International Journal of Advanced Manufacturing Technology*, vol. 129, no. 1–2, pp. 65–87, Sep. 2023, doi: 10.1007/s00170-023-12105-6.

[4] M. Elbah, H. Laouici, S. Benlahmidi, M. Nouioua, and Ma. Yallese, "Comparative assessment of machining environments (dry, wet and MQL) in hard turning of AISI 4140 steel with CC6050 tools," *The International Journal of Advanced Manufacturing Technology*, vol. 105, no. 5–6, pp. 2581–2597, Nov. 2019, doi: 10.1007/s00170-019-04403-9.

[5] R. Kumar, A. K. Sahoo, P. C. Mishra, R. K. Das, and M. Ukamanal, "Experimental investigation on hard turning using mixed ceramic insert under accelerated cooling environment," *International Journal of Industrial Engineering Computations*, pp. 509–522, Jan. 2018, doi: 10.5267/j.ijiec.2017.11.002.

[6] A. Çalık, O. Dokuzlar, and N. Uçar, "The effect of heat treatment on mechanical properties of 42CrMo4 steel," *Journal of Achievements of Materials and Manufacturing Engineering*, vol. 1, no. 98, pp. 5–10, Jan. 2020, doi: 10.5604/01.3001.0014.0811.

[7] C. Saikaew, P. Paengchit, and A. Wisitsoraat, "Machining performances of TiN+AlCrN coated WC and Al2O3+TiC inserts for turning of AISI 4140 steel under dry condition," *Journal of Manufacturing Processes*, vol. 50, pp. 412–420, Jan. 2020, doi: 10.1016/j.jmapro.2019.12.057.

[8] M. Kam and M. Şeremet, "Experimental investigation of the effect of machinability on surface quality and vibration in hard turning of hardened AISI 4140 steels using ceramic cutting tools," *Proceedings of the Institution of Mechanical Engineers Part E Journal of Process Mechanical Engineering*, vol. 235, no. 5, pp. 1565–1574, Apr. 2021, doi: 10.1177/09544089211007366.

[9] W. Ahmed, H. Hegab, A. Mohany, and H. Kishawy, "Analysis and Optimization of Machining Hardened Steel AISI 4140 with Self-Propelled Rotary Tools," *Materials*, vol. 14, no. 20, p. 6106, Oct. 2021, doi: 10.3390/ma14206106.

[10] S. Padhan *et al.*, "Investigation on Surface Integrity in Hard Turning of AISI 4140 Steel with SPPP-AlTiSiN Coated Carbide Insert under Nano-MQL," *Lubricants*, vol. 11, no. 2, p. 49, Jan. 2023, doi: 10.3390/lubricants11020049.

[11] İ. Asiltürk, M. Kuntoğlu, R. Binali, H. Akkuş, and E. Salur, "A Comprehensive Analysis of Surface Roughness, Vibration, and Acoustic Emissions Based on Machine Learning during Hard Turning of AISI 4140 Steel," *Metals*, vol. 13, no. 2, p. 437, Feb. 2023, doi: 10.3390/met13020437.

[12] M. A. Awadh, R. Kumar, O. İynen, M. Rafighi, M. Özdemir, and A. Pandey, "Machinability comparison of TICN-AL2O3-TIN, TIALN-TIN, and TIALSIN coated carbide inserts in turning hardened AISI 4340 steel using Grey-Crow Search Hybrid optimization," *Metals*, vol. 13, no. 5, p. 973, May 2023, doi: 10.3390/met13050973.

[13] S. R. Das, D. Dhupal, and A. Kumar, "Study of surface roughness and flank wear in hard turning of AISI 4140 steel with coated ceramic inserts," *Journal of Mechanical Science and Technology*, vol. 29, no. 10, pp. 4329–4340, Oct. 2015, doi: 10.1007/s12206-015-0931-2.

[14] S. K. Anand and S. Mitra, "Material Selection for Tool Holder using MCDM Methods," *International Journal of Emerging Technologies in Engineering Research (IJETER)*, vol. 9, no. 6, 2021.

[15] G. R. Chate *et al.*, "Sustainable machining: Modelling and optimization using Taguchi, MOORA and DEAR methods," *Materials Today Proceedings*, vol. 46, pp. 8941–8947, Jan. 2021, doi: 10.1016/j.matpr.2021.05.365.

[16] U. Ponugoti, N. S. S. Koka, and R. R. Dantuluri, "Multi objective optimization of process parameters in hard turning of AISI 52100 steel with surface irregularities using GRA-PCA," *Engineering Research Express*, vol. 5, no. 4, p. 045010, Sep. 2023, doi: 10.1088/2631-8695/acfc17.

[17] K. Safi, M. A. Yallese, S. Belhadi, T. Mabrouki, and A. Laouissi, "Tool wear, 3D surface topography, and comparative analysis of GRA, MOORA, DEAR, and WASPAS optimization techniques in turning of cold work tool steel," *The International Journal of Advanced Manufacturing Technology*, vol. 121, no. 1–2, pp. 701–721, May 2022, doi: 10.1007/s00170-022-09326-6.

[18] S. Hadjela, S. Belhadi, N. Ouelaa, K. Safi, and M. A. Yallese, "Straight turning optimization of low alloy steel using MCDM methods coupled with Taguchi approach," *The International Journal of Advanced Manufacturing Technology*, vol. 124, no. 5–6, pp. 1607–1621, Dec. 2022, doi: 10.1007/s00170-022-10584-7.

[19] P. Umamaheswarrao, D. R. Raju, K. Suman, and B. R. Sankar, "Multi objective optimization of process parameters for hard turning of AISI 52100 steel using Hybrid GRA-PCA," *Procedia Computer Science*, vol. 133, pp. 703–710, Jan. 2018, doi: 10.1016/j.procs.2018.07.129.

[20] F. Khelfaoui, M. A. Yallese, S. Boucherit, H. Boumaaza, and N. Ouelaa, "Minimizing tool wear, cutting temperature and surface roughness in the intermittent turning of AISI D3 steel using the DF and GRA method," *Tribology in Industry*, vol. 45, no. 1, pp. 89–101, Mar. 2023, doi: 10.24874/ti.1395.10.22.01.

[21] G. Meral, M. Sarıkaya, M. Mia, H. Dilipak, U. Şeker, and M. K. Gupta, "Multi-objective optimization of surface roughness, thrust force, and torque produced by novel drill geometries using Taguchi-based GRA," *The International Journal of Advanced Manufacturing Technology*, vol. 101, no. 5–8, pp. 1595–1610, Nov. 2018, doi: 10.1007/s00170-018-3061-z.

[22] P. B. Patole and V. V. Kulkarni, "Experimental investigation and optimization of cutting parameters with multi response characteristics in MQL turning of AISI 4340 using nano fluid," *Cogent Engineering*, vol. 4, no. 1, p. 1303956, Jan. 2017, doi: 10.1080/23311916.2017.1303956.

[23] N. N. M. I. Elsiti and N. M. H. S. Elmunafi, "Optimization of machining parameters for turning process by using grey relational analysis," *World Journal of Advanced Research and Reviews*, vol. 17, no. 1, pp. 756–761, Jan. 2023, doi: 10.30574/wjarr.2023.17.1.0080.

[24] P. M. Rao, Ch. D. Raj, S. H. Dhoria, M. Vijaya, and J. R. R. Chowdary, "Multi-Objective optimization of turning for Nickel-Based alloys using Taguchi-GRA and TOPSIS approaches," *Journal of the Institution of Engineers (India) Series D*, vol. 105, no. 3, pp. 1473–1484, Oct. 2023, doi: 10.1007/s40033-023-00554-y.

[25] Mst. N. Sultana and N. R. Dhar, "Hybrid GRA-PCA and modified weighted TOPSIS coupled with Taguchi for multi-response process parameter optimization in turning AISI 1040 steel," *Archive of Mechanical Engineering*, pp. 23–49, Jan. 2020, doi: 10.24425/ame.2020.131707.

[26] R. Kumar, A. K. Sahoo, P. C. Mishra, and R. K. Das, "Comparative study on machinability improvement in hard turning using coated and uncoated carbide inserts: part II modeling, multi-response optimization, tool life, and economic aspects," *Advances in Manufacturing*, vol. 6, no. 2, pp. 155–175, Mar. 2018, doi: 10.1007/s40436-018-0214-0.

[27] V. V. Upadhyay, "Machining Parameters Optimization by Grey Relational Analysis of Alloy Steel AISI 4140," *PalArch's Journal of Archaeology of Egypt/Egyptology*, vol. 17, no. 7, pp. 4107–4121, 2020.

[28] S. Yaqoob, J. A. Ghani, N. Jouini, A. Z. Juri, C. H. C. Haron, and C. Hassan, "Multi-objective optimization using Grey Relational Analysis (GRA) for the high-speed orthogonal turning of heat-treated alloy steel," *J. Tribol.*, vol. 43, pp. 1–16, 2024.

[29] N. Y. R. Reddy, "Optimization of surface roughness and material removal rate in turning using gray-based Taguchi approach," *World Journal of Advanced Engineering Technology and Sciences*, vol. 9, no. 1, pp. 364–371, Jun. 2023, doi: 10.30574/wjaets.2023.9.1.0183.

[30] S. N. Hong and U. V. T. Nhu, "Multi-objective optimization in turning operation of AISI 1055 steel using DEAR method," *Tribology in Industry*, vol. 43, no. 1, pp. 57–65, Mar. 2021, doi: 10.24874/ti.1006.11.20.01.

[31] V. R. Pathapalli, S. R. Pittam, V. Sarila, D. Burragalla, and A. Gagandeep, "Multi-objective parametric optimization of AWJM process using Taguchi-based GRA and DEAR methodology," *Proceedings of the Institution of Mechanical Engineers Part E Journal of Process Mechanical Engineering*, vol. 238, no. 6, pp. 2845–2853, Apr. 2023, doi: 10.1177/09544089231164836.

[32] M. Imran, S. Suo, Y. Bai, Y. Wang, and R. Naveed, "'Optimising subsurface integrity and surface Quality in Mild Steel Turning: A Multi-Objective Approach to tool wear and Machining Parameters,'" *Journal of Materials Research and Technology*, Feb. 2025, doi: 10.1016/j.jmrt.2025.01.246

[33] X. Tian, J. Zhao, W. Qin, F. Gong, Y. Wang, and H. Pan, "Performance of ceramic tools in high-speed cutting iron-based superalloys," *Machining Science and Technology*, vol. 21, no. 2, pp. 279–290, Apr. 2017, doi: 10.1080/10910344.2017.1284559.

[34] Mitutoyo Corporation, *Surftest SJ-210 / SJ-310 Series – Portable Surface Roughness Tester*, Document technique PRE1533, 2020. [On line]. Available: https://shop.mitutoyo.eu/media/mitutoyoData/DO/base/PRE%201533%20-%20SJ-210%2C310%20SERIES_WEB.pdf

[35] F. Zhujani, G. Todorov, K. Kamberov, and F. Abdullahu, "Mathematical modeling and optimization of machining parameters in CNC turning process of Inconel 718 using the Taguchi method," *Journal of Engineering Research*, Oct. 2023, doi: 10.1016/j.jer.2023.10.029.

[36] Sandvik Coromant, Ceramics - Productive and intelligent machining of refractory superalloys, 2010.

[37] D. P. Selvaraj, P. Chandramohan, and M. Mohanraj, "Optimization of surface roughness, cutting force and tool wear of nitrogen alloyed duplex stainless steel in a dry turning process using Taguchi method," *Measurement*, vol. 49, pp. 205–215, Dec. 2013, doi: 10.1016/j.measurement.2013.11.037.

[38] L. G. P. De Souza, J. E. M. Gomes, É. M. Arruda, G. Silva, A. P. De Paiva, and J. R. Ferreira, "Evaluation of trade-off between cutting time and surface roughness robustness regarding tool wear in hard turning finishing," *The International Journal of Advanced Manufacturing Technology*, vol. 123, no. 9–10, pp. 3047–3078, Nov. 2022, doi: 10.1007/s00170-022-10354-5.

[39] A. Zerti, M. A. Yallese, I. Meddour, S. Belhadi, A. Haddad, and T. Mabrouki, "Modeling and multi-objective optimization for minimizing surface roughness, cutting force, and power, and maximizing productivity for tempered stainless steel AISI 420 in turning operations," *The International Journal of Advanced Manufacturing Technology*, vol. 102, no. 1–4, pp. 135–157, Dec. 2018, doi: 10.1007/s00170-018-2984-8.

[40] G. E. García, F. Trigos, D. Maldonado-Cortés, and L. Peña-Parás, "Optimization of surface roughness on slitting knives by titanium dioxide nano particles as an additive in grinding lubricant," *The International Journal of Advanced Manufacturing Technology*, vol. 96, no. 9–12, pp. 4111–4121, Mar. 2018, doi: 10.1007/s00170-018-1834-z.

[41] F. Trigos, D. Maldonado-Cortés, L. Peña-Parás, and G. E. García, "Influence of coating chemical composition and thickness layer on the wear behavior of cutting tools A business analytics approach," *Tribology in Industry*, vol. 41, no. 2, pp. 286–291, Jun. 2019, doi: 10.24874/ti.2019.41.02.14.

[42] T. M. Thobane, S. K. Chaubey, and K. Gupta, "Analysis of Tool Wear and Chip Morphology during Turning of AZ31B Magnesium Alloy under Dry Environment," *Journal of Manufacturing and Materials Processing*, vol. 7, no. 5, p. 187, Oct. 2023, doi: 10.3390/jmmp7050187.

[43] C. Saikaew, P. Paengchit, and A. Wisitsoraat, "Machining performances of TiN+AlCrN coated WC and Al2O3+TiC inserts for turning of AISI 4140 steel under dry condition," *Journal of Manufacturing Processes*, vol. 50, pp. 412–420, Jan. 2020, doi: 10.1016/j.jmapro.2019.12.057.

[44] R. N. Marigoudar and K. Sadashivappa, "Comparison of tool life and surface characteristics of uncoated, coated carbide and ceramic tools during machining of SiC reinforced ZA43 alloy MMC," *Materials Science and Technology*, vol. 30, no. 8, pp. 876–887, Jan. 2014, doi: 10.1179/1743284713y.0000000484.

[45] R. Kumar, A. K. Sahoo, P. C. Mishra, and R. K. Das, "Investigation on tool wear and surface characteristics in hard turning under Air-Water jet spray impingement cooling environment," *Tribology in Industry*, vol. 41, no. 2, pp. 172–187, Jun. 2019, doi: 10.24874/ti.2019.41.02.04.

[46] M. V. Lungu *et al.*, "Evaluation of magnetron sputtered TIALSIN-Based thin films as protective coatings for tool steel surfaces," *Coatings*, vol. 14, no. 9, p. 1184, Sep. 2024, doi: 10.3390/coatings14091184

[47] G. Zheng, G. Zhao, X. Cheng, R. Xu, J. Zhao, and H. Zhang, "Frictional and wear performance of TiAlN/TiN coated tool against high-strength steel," *Ceramics International*, vol. 44, no. 6, pp. 6878–6885, Jan. 2018, doi: 10.1016/j.ceramint.2018.01.113.

[48] F. Molaiekiya, M. Aramesh, and S. C. Veldhuis, "Chip formation and tribological behavior in high-speed milling of IN718 with ceramic tools," *Wear*, vol. 446–447, p. 203191, Jan. 2020, doi: 10.1016/j.wear.2020.203191.

[49] K. N. Mwangi, J. Wambua, F. M. Mwema, J. M. Wakiru, and T.-C. Jen, "Evaluation of surface quality and productivity in conventional milling of copper beryllium using minimum quantity lubrication," *Tribology in Industry*, vol. 3, no. 46, pp. 355–367, Sep. 2024, doi: 10.24874/ti.1566.10.23.01.

[50] F. Zhujani, F. Abdullahu, G. Todorov, and K. Kamberov, "Optimization of multiple performance characteristics for CNC turning of Inconel 718 using Taguchi–Grey relational approach and analysis of variance," *Metals*, vol. 14, no. 2, p. 186, Feb. 2024, doi: 10.3390/met14020186.

[51] S. Haoues, M. A. Yallese, S. Belhadi, S. Chihaoui, and A. Uysal, "Modeling and optimization in turning of PA66-GF30% and PA66 using multi-criteria decision-making (PSI, MABAC, and MAIRCA) methods: a comparative study," *The International Journal of Advanced Manufacturing Technology*, vol. 124, no. 7–8, pp. 2401–2421, Dec. 2022, doi: 10.1007/s00170-022-10583-8.

[52] T. P. Jeevan and S. R. Jayaram, "Performance evaluation of Jatropha and Pongamia oil based environmentally friendly cutting fluids for turning AA 6061," *Advances in Tribology*, vol. 2018, pp. 1–9, Jan. 2018, doi: 10.1155/2018/2425619.

[53] B. Wang *et al.*, "Advancements in material removal mechanism and surface integrity of high speed metal cutting: A review," *International Journal of Machine Tools and Manufacture*, vol. 166, p. 103744, May 2021, doi: 10.1016/j.ijmachtools.2021.103744.

[54] N. S. Narayanan, N. Baskar, M. Ganesan, M. P. Jenarthanan, and S. Praveen, "Evaluation and optimization of surface roughness and metal removal rate through RSM, GRA, and TOPSIS techniques in turning PTFE polymers," in *Lecture notes in mechanical engineering*, 2019, pp. 595–605. doi: 10.1007/978-981-13-6374-0_65.

[55] F. Abdullahu, F. Zhujani, G. Todorov, and K. Kamberov, "An Experimental Analysis of Taguchi-Based Gray Relational Analysis, Weighted Gray Relational Analysis, and Data Envelopment Analysis Ranking Method Multi-Criteria Decision-Making Approaches to Multiple-Quality Characteristic Optimization in the CNC Drilling Process," *Processes*, vol. 12, no. 6, p. 1212, Jun. 2024, doi: 10.3390/pr12061212.

[56] S. Chakraborty, H. N. Datta, and S. Chakraborty, "Grey Relational Analysis-Based Optimization of Machining Processes: a Comprehensive Review," *Process Integration and Optimization for Sustainability*, vol. 7, no. 4, pp. 609–639, Jan. 2023, doi: 10.1007/s41660-023-00311-4.

[57] D. Pendokhare and S. Chakraborty, "A review on multi-objective optimization techniques of wire electrical discharge machining," *Archives of Computational Methods in Engineering*, Oct. 2024, doi: 10.1007/s11831-024-10195-3.

[58] S. Kumar, Y. Rizvi, and R. Kumar, "A Review of Modelling and Optimization Techniques in Turning Processes," *International Journal of Mechanical Engineering and Technology (IJMET)*, vol. 9, no. 3, pp. 1146–1156, Mar. 2018. [On line]. Available: https://iaeme.com/MasterAdmin/Journal_uploads/IJMET/VOLUME_9_ISSUE_3/IJMET_09_03_118.pdf

[59] P. B. Zaman, M. N. Sultana, and N. R. Dhar, "Multi-variant hybrid techniques coupled with Taguchi in multi-response parameter optimisation for better machinability of turning alloy steel," *Advances in Materials and Processing Technologies*, vol. 8, no. 3, pp. 3127–3147, Jul. 2021, doi: 10.1080/2374068x.2021.1945302.

[60] S. Haoues, M. A. Yallese, M. Kaddeche, A. Uysal, and K. Safi, "Investigation on machining of GFRP through ANOVA, DFA, and CoCoSo method combined with Taguchi approach," *Journal of Reinforced Plastics and Composites*, Mar. 2024, doi: 10.1177/07316844241239249.

[61] K. Malik *et al.*, "The hybridization effects of glass and carbon fibers on the mechanical properties of KENAF Mat/Epoxy composites," *Journal of Natural Fibers*, vol. 19, no. 17, pp. 15432–15447, Oct. 2022, doi: 10.1080/15440478.2022.2127437.

[62] M. Kumar and H. Singh, "Multi response optimization in wire electrical discharge machining of Inconel X-750 using Taguchi's technique and grey relational analysis," *Cogent Engineering*, vol. 3, no. 1, p. 1266123, Dec. 2016, doi: 10.1080/23311916.2016.1266123.

[63] M. Brn, R. Beedu, J. P. K, and S. R. Potti, "Study on Machining Quality in Abrasive Water Jet Machining of Jute-Polymer Composite and Optimization of Process Parameters through Grey Relational Analysis," *Journal of Composites Science*, vol. 8, no. 1, p. 20, Jan. 2024, doi: 10.3390/jcs8010020.

[64] N. Senthilkumar, V. Selvakumar, and T. Tamizharasan, "Optimization and Performance Analysis of Uncoated and Coated Carbide Inserts during Hard Turning AISI D2 Steel Using Hybrid GRA-PCA Technique," *Applied Mechanics and Materials*, vol. 852, pp. 151–159, Sep. 2016, doi: 10.4028/www.scientific.net/AMM.852.151.

## Nomenclature

| **Control variables** | | | |
|---|---|---|---|
| **Vc** | Cutting speed | **Doc (mm)** | Depth of cut |
| **F(mm/rev)** | Feed rate | **Ti** | Tool material |
| **Output variables** | | | |
| **Ra (μm)** | Surface roughness | **VB** | Flank wear |
| **CE (%)** | Circularity error | **S/N** | Signal to noise |
| **MRR ($mm^3$/min)** | Material removal rate | **DEAR** | Data envelopment-based ranking |
| **GRA** | Grey relation analysis | **GRG** | Grey relation grade |
| **MOORA** | Multi-objective optimization by ratio analysis | **MS** | Mean squares |
| **SS** | Sum of squares | **DF** | Degree of freedom |